Article

Physical and Chemical Foam Injection Moulding of Natural-Fibre-Reinforced Polypropylene—Assessment of Weight-Reduction Potential and Mechanical Properties

Matthias Mihalic [1] , **Claudia Pretschuh** [1] , **Thomas Lummerstorfer** [2] **and Christoph Unterweger** [1,*]

[1] Wood K Plus—Kompetenzzentrum Holz GmbH, Altenberger Strasse 69, 4040 Linz, Austria
[2] Borealis Polyolefine GmbH, St. Peter Strasse 25, 4021 Linz, Austria
* Correspondence: c.unterweger@wood-kplus.at; Tel.: +43-732-2468-6758

Abstract: Reducing weight not only consumes fewer resources for manufacturing but also requires less energy for transportation, thus preserving resources and reducing CO_2 emissions. The latter part is of utmost importance in mobility applications. For example, in the automotive industry, the large-scale production of lightweight structural parts is becoming a main issue. An effective method to meet these requirements is foam injection moulding. In this study, physical (MuCell technology) and chemical foam injection moulding was used to produce plates made from wood-fibre- and cellulose-fibre-reinforced polypropylene, respectively. For both technologies, the used core-back method enabled precise mould opening during injection and thus allowed for variation in the plate thickness and density. The simpler short-shot technology, used only for the chemical foaming trials with differing shot volumes, provided plates with constant thicknesses. The foam structure and finally the mechanical properties of the plates depended on the filler type, the foaming method and the density. The latter was directly linked to either the plate thickness or the shot volume. Physical foaming appeared to be slightly more effective regarding the achievable density reduction (up to 37% reduction), but the physically foamed parts had worse mechanical properties at equal density than their chemically foamed counterparts. Besides the comparison of different foaming methods, this study provides the tensile, flexural and impact properties of natural-fibre-reinforced polypropylene composites over a wide density range, thus offering a good basis for evaluating weight-saving potential for various applications.

Keywords: foam injection moulding; natural fibre composite; weight reduction; polypropylene

1. Introduction

Lightweight design is a key focus in the automotive industry to lower vehicle fuel consumption, thereby reducing CO_2 emissions and contributing to more sustainable mobility. As a reduction in weight is usually accompanied by decreasing performance, the production of lightweight structural parts is not an easy task. Methods yielding high weight reductions with low trade-offs in terms of mechanical performance have to be found while maintaining high output and low costs. Among other possibilities, foam injection moulding is an effective method to meet these requirements, but systematic investigations of the process parameters involved and databases for evaluating its weight-saving potential are limited.

Further reductions in the weight of parts can be achieved by substituting conventional mineral fillers such as talc or glass fibres for natural fibres due to the lower density of the latter [1]. The mechanical properties of natural-fibre-reinforced composites (NFCs) are comparable to their mineral-filled counterparts [2], and they bear the potential for a reduction in greenhouse gas emissions [3,4]. Such composites are increasingly being used in automotive interior applications, such as in door panels and dashboards [5]. The suitability of standard modifiers for tuning the mechanical properties of NFCs and their potential use

in automotive interior applications have been shown in a previous study [6]. Furthermore, the presence of filler particles has been shown to improve the foaming behaviour of these compounds since the particles act as nucleating sites for foam cell formation, resulting in a higher cell density and a reduced cell size [7,8]. However, care must be taken to ensure a homogeneous distribution of the fillers in the matrix, since agglomeration of the fibres may negatively affect the foam quality [9].

Foam injection moulding (FIM) can, in general, be divided into two main categories based on the nature of the foaming agent—physical or chemical. Physical foaming, also known as microcellular injection moulding [10], is typically achieved in a four-step process via homogeneously dissolving a supercritical gas (such as N_2 or CO_2) in a polymer melt, which is followed by cell nucleation and then cell expansion when the melt reaches the mould cavity, where a rapid pressure drop occurs, and finally cell stabilisation [11,12]. Microcellular injection moulding is often used synonymously with the MuCell® process, which is where the supercritical fluid is injected into the melt in the plastification zone [13]. Another method to achieve physical foaming is the supercritical-gas-laden pellet injection moulding (SIFT) process [14,15], where plastic pellets are first loaded with CO_2 before being fed into the injection moulding machine.

In contrast to physical foaming, chemical foaming is achieved by gas formation, which occurs by the decomposition of a chemical blowing agent [16] when the melt reaches a certain temperature. While chemical foaming has the advantage that it can be performed basically with conventional injection moulding equipment (only a shut-off nozzle is required), its main drawbacks are typically a less homogeneous bubble formation and the potential problems caused by the chemical by-products of the blowing agent [9,17], such as degradation of the polymer matrix, reduced mechanical properties or contamination of the mould surface, [18], as well as a decreased thermal stability [15]. Whether chemical or physical foaming is the preferred method depends mainly on the type of material, the geometry of the injection-moulded parts and the machine utilisation rate, i.e., the rate of material consumption. Chemical foaming tends to be favourable for unfilled polymers (because the blowing agent itself can act as a nucleating site [19]), at rather high wall thicknesses ($\geq$4 mm) and at low material consumption/low machine utilisation. Physical foaming is, in contrast, typically preferable for parts with thin walls ($\leq$2 mm) and at high material consumption/high machine utilisation rates. In addition, physical foaming allows for a wider processing temperature window and has a higher weight-reduction potential [20].

Another possible distinction of the available methods for foam injection moulding is based on the manner in which the mould is filled [21]: in low-pressure FIM, also known as "short-shot" FIM, the mould is partially filled with the gas-loaded melt, whereupon the expansion of the gas results in the mould becoming fully filled. In contrast, in the case of high-pressure FIM ("core-back", "breathing mould" or "full shot" FIM), the gas-loaded melt is injected until the mould is fully filled, and the mould is subsequently opened partially, which triggers the expansion of the gas and the formation of a foamed structure. While short-shot FIM is easier to set up and does not require specific equipment, it has been demonstrated that the rapid pressure drop induced by the mould opening in core-back FIM facilitates cell nucleation and thus allows for higher cell fractions, a higher level of weight reduction and an improved stiffness-to-weight ratio [7,10,22,23].

Regardless of the method—physical or chemical FIM—the foamed parts typically exhibit a layered structure, with a foamed core layer being sandwiched between two solid skin layers [13]. This sandwich structure may result in improved specific modulus and strength values compared to solid parts [7,8,24]. Besides the obvious benefit of a reduced part weight, a further advantages of foam injection moulding compared to compact injection moulding is that it involves a reduced melt viscosity, which leads to reduced injection pressures, the possibility of using lower processing temperatures and a reduction in cycle times [25–28]. In addition, foamed parts show superior acoustic and thermal insulation properties than their compact counterparts [9]

The aim of the present study was to systematically evaluate different foam injection moulding methods regarding their weight reduction potential and achievable mechanical property profiles. Physical and chemical foaming, each with different mould opening gaps, i.e., different part thicknesses and, thus, different degrees of foaming, were investigated for two NFCs, wood-fibre- and cellulose-fibre-reinforced polypropylene.

2. Materials and Methods

2.1. Materials

The materials used for this study were a commercial wood reinforced PP composite ("PPWood") from Borealis AG and a self-made cellulose-reinforced PP composite ("PPCell"). The base polymer in both cases was a heterophasic PP copolymer (PP-HECO) from Borealis AG with a melt flow rate (MFR) of 100 g/10 min (230 °C, 2.16 kg). PP-Wood contained 20 wt% of roughly cubic-shaped softwood fibres with a particle size in the 70–150 μm range and an L/D ratio of approx. 1.5 [29]. PPCell contained 20 wt% of regenerated cellulose fibres with a nominal length of 300 μm and a diameter of 10 μm. Both compounds contained 2 wt% of a maleic-anhydride-grafted PP (MA-PP) as a coupling agent. The PPCell compound was prepared at Wood K plus using a Brabender DSE20/40D twin screw extruder with a 20 mm screw diameter, where the polymer and the coupling agent were fed at the hopper, and the fibres were fed via a twin-screw sidefeeder (D = 20 mm) attached at position 11D, i.e., after the plastification zone. A throughput of 10 kg/h and a screw speed of 375 rpm were chosen. A decreasing temperature profile ranging from 210 °C in the melting zone to 180 °C at the die was used in order to keep thermal degradation of the fibres to a minimum. All materials were dried overnight at 80 °C prior to injection moulding.

2.2. Injection Moulding

2.2.1. Physical Foaming

Physical foaming was achieved by nitrogen injection according to the MuCell® process. The trials were carried out at ENGEL Austria GmbH using a hydraulic/hybrid ENGEL Duo 12060/1700 injection moulding machine with a 120 mm screw diameter. The temperature profile increased from 180 °C in the melting zone to 200 °C at the nozzle. Tool temperatures of 60 °C ("T60") and 40 °C ("T40") were used. After the initial gas loading of 0.3 wt% of N_2 in the melt ("N03") resulted in insufficient cavity filling at larger mould opening gaps, the loading was increased to 0.6 wt% ("N06") for all remaining trials.

A plate tool of an 800 × 400 mm^2 area with three gates distributed along the central "axis" of the plates was used. The nominal thickness of the plate tool was 2.5 mm; for the core-back trials, opening gaps of 0/0.1/0.2/0.3/0.4/0.5/0.75/1 mm were used, resulting in nominal plate thicknesses ranging from 2.5 mm to 3.5 mm. The specimens for the mechanical and microscopic characterisations were milled out of the plates using a CNC machine according to the sketch shown in Figure 1.
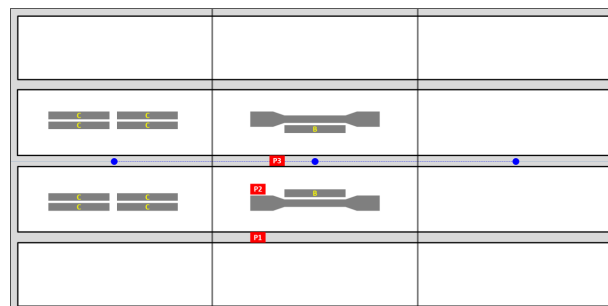

Figure 1. Plate geometry used for the physical foaming trials. Blue dots indicate injection points. Specimens for bending test (marked "B", 80 × 10 mm^2) and tensile test, as well as Charpy impact test (marked "C", 80 × 10 mm^2), are shown in dark grey. Specimens for density test and optical microscopy (marked P1, P2, P3", 20 × 15 mm^2) are shown in red.
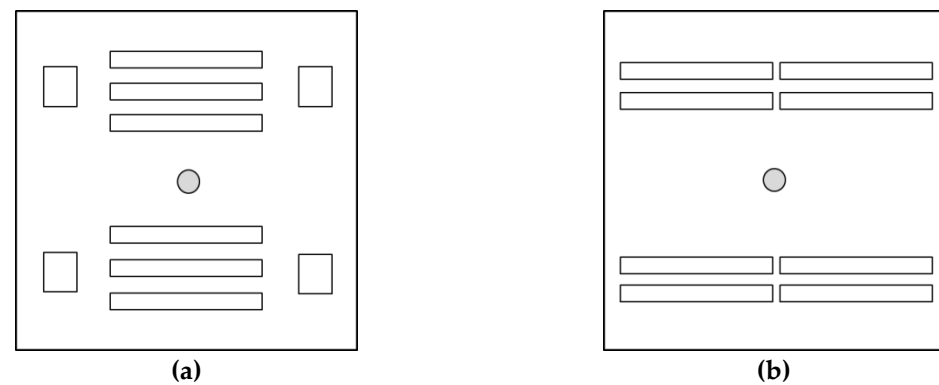
2.2.2. Chemical Foaming

The chemical foaming trials were performed using a Wittmann Battenfeld SmartPower 120 servo-hydraulic injection moulding machine with a 35 mm screw diameter and a 120 kN clamping force. The temperature profile increased from 145 °C near the hopper to 190 °C at the nozzle. Foaming was achieved by adding 3 wt% of a chemical blowing agent Hydrocerol$^®$ ITP845 by Clariant Masterbatches GmbH (Vienna, Austria) via an automatic dosing unit. Besides the core-back ("CB") foaming trials with mould opening gaps of 0/0.2/0.4/0.8/1 mm (resulting in plate thicknesses ranging from 3 mm to 4 mm), additional trials in short-shot mode ("SSh") with dosage volumes of 100%/95%/90% of the switchover volume were carried out.

The majority of the chemical foaming trials were performed using a $200 \times 150 \times 3$ mm^3 plate tool with a wedge-shaped film gate (Figure 2). Evidently, this geometry led to a different melt flow pattern than that of the geometry of the plates used for the physical foaming. Therefore, in order to investigate the influence of the gate geometry on the properties of the foamed specimens, additional core-back trials were performed using a $180 \times 180 \times 3$ mm^3 plate tool with a central gate (Figure 3).
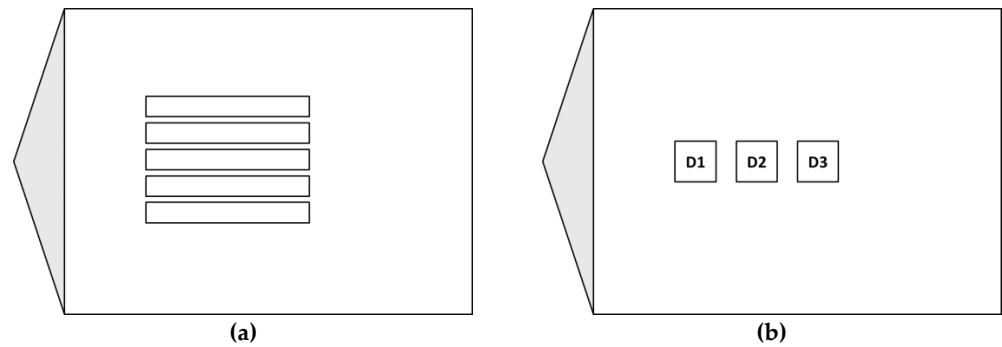
Figure 2. Geometry of the film gate plates used for the short-shot and core-back chemical foaming trials. Sampling positions are shown for flexural and impact testing (80×10 mm^2) (**a**) and for density measurements and microscopy (20×20 mm^2) (**b**).

Figure 3. Geometry of the central gate plates used for additional core-back chemical foaming trials. Sampling positions are shown for flexural testing (80×10 mm^2) and density measurements (20×20 mm^2) (**a**) and for impact testing (80×10 mm^2) (**b**).

2.3. Characterisation of the Injection-Moulded Samples

Density measurements were performed according to the Archimedes principle following EN ISO 1183-1 using a Sartorius YDK01 density kit and an analytical balance. The flexural properties were determined via a 3-point bending test according to EN ISO 178 using a Messphysik Beta 50 universal testing machine with a preload force of 5 N and a test speed of 2 mm/min. The notched and unnotched Charpy impact strengths according to EN ISO 179 were characterised using a CEAST 9050 pendulum impact tester with a 0.5 J

pendulum hammer for the notched samples and a 2 J or 7.5 J hammer, depending on the impact strength, for the unnotched samples.

Tensile tests according to EN ISO 527 were performed on the physically foamed samples using a Messphysik Beta 20-10 universal testing machine with a preload force of 3 N and a test speed ranging from 1 mm/min (for the determination of Young's modulus) to 50 mm/min (for the determination of the tensile strength). No such test was performed on the chemically foamed samples as the plates produced were not large enough to produce standardised shoulder bars.

In addition to the mechanical characterisation, the foam structure was analysed via optical microscopy of the cross-sections of the foamed samples using an Olympus BX-RLA2 reflected light microscope. For this purpose, the specimens were embedded in epoxy resin and afterwards were smoothed and polished with sandpaper with increasingly fine grit sizes, finishing with a special polishing cloth and polishing suspension.

3. Results and Discussion

3.1. Mechanical Properties

3.1.1. Physical Foaming Trials

Density versus Plate Thickness

Figure 4 shows a correlation of the densities of the foamed samples, which were taken from the plates at position P2 (cf. Figure 1), with the nominal plate thickness. Both the materials showed roughly the same trend of their density-versus-thickness curves. There was a drop in the density of approx. 10% from the compact samples to the foamed samples at equal thickness. The density of the foamed samples at the maximum thickness (3.5 mm) was approx. 30% lower (ranging from 28.6% to 30.8%) than that at the minimum thickness (2.5 mm) in all cases, which is similar to the relative difference in thickness (28.6%). Assuming a constant part weight for all the samples, a reciprocal correlation between the density and the part thickness can be expected; this was roughly the case for all the foamed specimens. In addition, the following observations were made:

- In the compact specimens and at low foaming degrees (small mould opening gaps), the absolute density of PPWood was slightly lower than the density of PPCell. At higher foaming degrees (large mould opening gaps), this difference became negligible.
- A lower gas loading resulted in a higher density, indicating a lower foaming degree (see the curve of PPCell_N03_T60 in Figure 4).
- The influence of the tool temperature on the density-versus-thickness curve was negligible for PPCell, whereas for PPWood, slightly lower densities were achieved at a 40 °C tool temperature than at 60 °C (except for an outlier at a thickness of 2.6 mm).


The inset equation in the figure reads:

$$y = 2.174x^{-1.003}$$
$$R^2 = 0.932$$
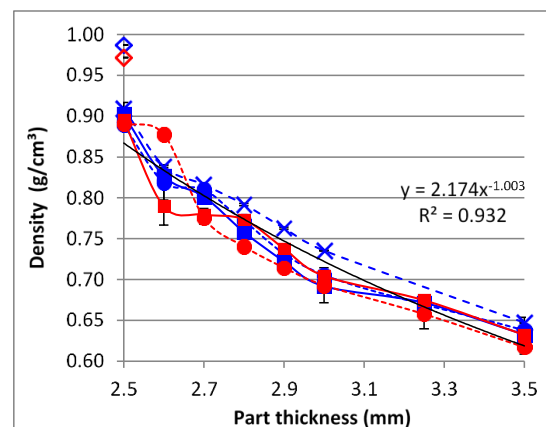
Figure 4. Dependence of the part density on the nominal part thickness. Legend: PPCell, PPWood. Compact samples—◇◇; samples N03_T60—✕✕, dashed line; samples N06_T60—■■, solid lines; samples N06_T40—●●, dotted lines. Error bars show 95% confidence interval. If not visible, error bars lie within the size of the used symbol for the respective sample.

Tensile and Flexural Properties

Both materials showed a linear dependency of the tensile modulus and strength on the density; this trend also extended to the compact samples. There was no noticeable influence of the gas loading and tool temperature on the tensile modulus and strength. While both materials showed very similar values for the tensile modulus (cf. Figure 5, left) in relation to the density, the PPCell compound was clearly superior to the PPWood compound in terms of the tensile strength (cf. Figure 5, right). This indicates the effect of the aspect ratio of the fibres, which was approx. 30 in the case of the cellulose fibres in PPCell and approx. 1.5 in the case of the wood particles in PPWood. The effect of the fibre aspect ratio on the mechanical properties has been shown in the literature [30]. The flexural modulus (cf. Figure 6, left) and strength (cf. Figure 6, right) followed the same trends as the respective tensile properties; this was the case for all the samples. However, the flexural data, particularly the modulus, showed a significant amount of scattering, which made it difficult to assess any possible influence of the processing conditions or even the filler type.
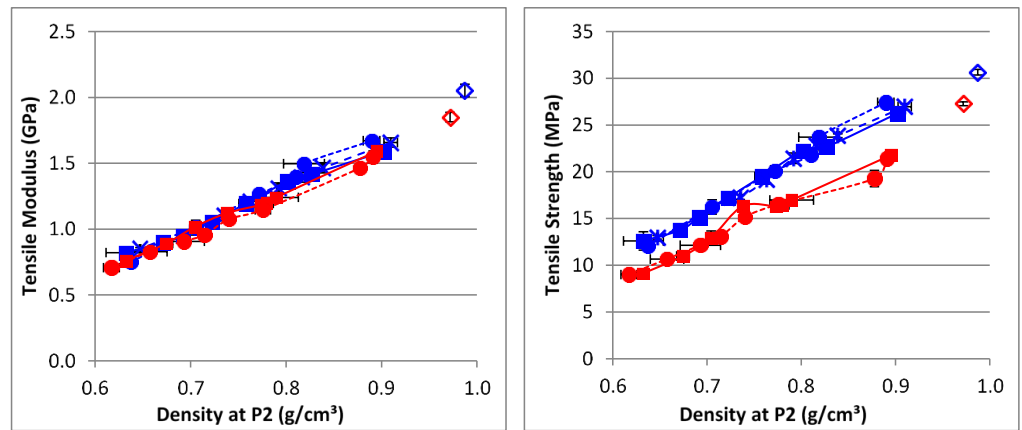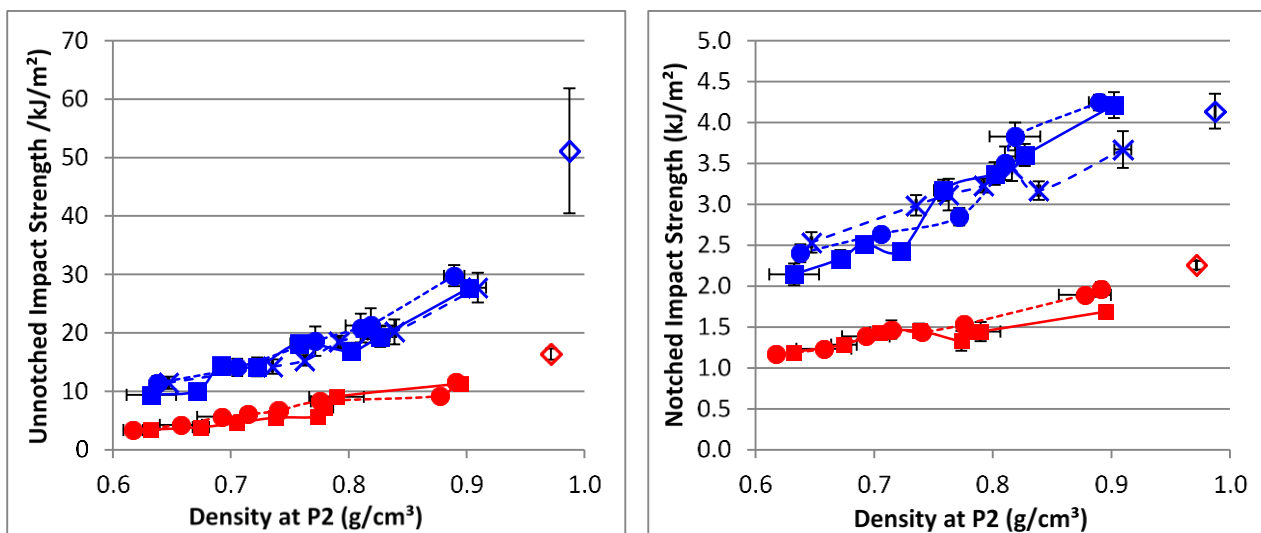

Figure 5. Dependence of the tensile modulus (**left**) and tensile strength (**right**) on the density of the foamed parts. Legend: PPCell, PPWood. Compact samples—◇◇; samples N03_T60—✕, dashed line; samples N06_T60—■■, solid lines; samples N06_T40—●●, dotted lines. Error bars show 95% confidence interval. If not visible, error bars lie within the size of the used symbol for the respective sample.
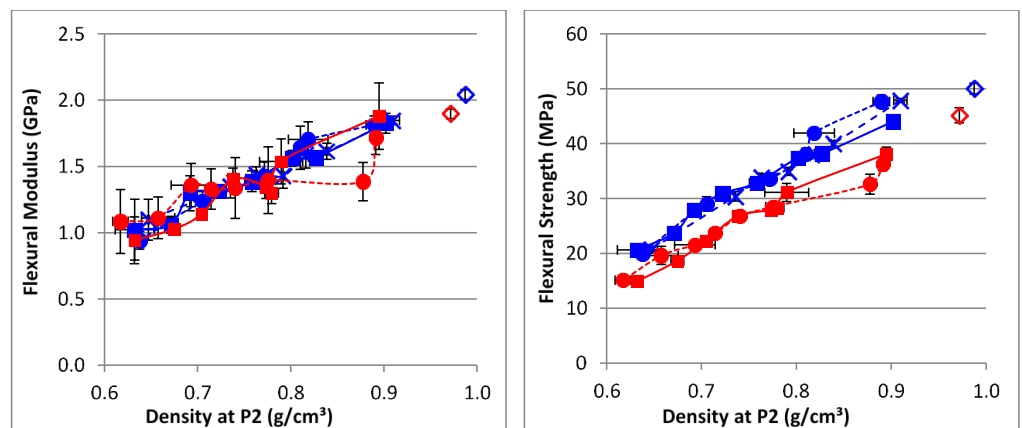
Figure 6. Dependence of the flexural modulus (**left**) and flexural strength (**right**) on the density of the foamed parts. Legend: PPCell, PPWood. Compact samples—◇◇; samples N03_T60—✕, dashed line; samples N06_T60—■■, solid lines; samples N06_T40—●●, dotted lines. Error bars show 95% confidence interval. If not visible, error bars lie within the size of the used symbol for the respective sample.

Impact Properties

Figure 7 shows the unnotched (left) and notched (right) Charpy impact strength of PPWood and PPCell as a function of the density. The observed trends for the impact behaviour differed from the tensile and flexural properties in several aspects: While the discrepancy between the two materials was almost negligible for the tensile and flexural modulus and in the range of 25–30% in favour of PPCell in the tensile and flexural strength, the differences in the impact properties were much more significant—roughly 250–300% in the unnotched impact strength and around 100% in the notched impact strength, both in favour of PPCell. There was again a roughly linear correlation between the notched impact strength and the density, albeit with some scattering, which also extended to the compact samples. In contrast, the dependency of the unnotched impact strength on the density was not quite linear but appeared to become steeper with a higher density, i.e., lower degree of foaming. In particular, there was a significant drop in the unnotched impact strength of both materials going from the compact samples to the respective foamed samples at equal thicknesses, i.e., without mould opening (approx. −45% for PPCell and approx. −30% for PPWood). The large confidence interval of the unnotched impact strength of the compact PPCell sample should be given special consideration here because (a) the result seems to be valid, since the raw data did not contain any statistical outliers, and (b) it was the only sample with such a large amount of scattering. It should also be noted that this occurred only in the PPCell sample, which contained fibres with an aspect ratio of approx. 30, and not in the PPWood sample, whose filler particles were nearly cubic. Considering in addition that the position of the impact testing specimens in the injection-moulded plates in relation to the position of the gate (cf. Figure 1) resulted in a non-uniform flow direction, one can conclude that this scattering was the result of a non-uniform fibre orientation in the PPCell sample and that such orientation effects were significant in the compact samples but played only a minor role in the foamed samples. The latter observation is in accordance with the literature, where it has been demonstrated that the expansion of the foam cells results in fibre displacement in terms of both translation and rotation [31].


Figure 7. Dependence of the Charpy unnotched (**left**) and notched impact strength (**right**) on the density of the foamed parts. Legend: PPCell, PPWood. Compact samples—◇◇; samples N03_T60—✕, dashed line; samples N06_T60—■■, solid lines; samples N06_T40—●●, dotted lines. Error bars show 95% confidence interval. If not visible, error bars lie within the size of the used symbol for the respective sample.

Similar to the tensile and flexural properties, no clear statement could be made regarding the influence of the gas loading and tool temperature on the impact properties in

relation to the density, as the observed differences were small and in the same range as the 95% confidence intervals of the measured values.

3.1.2. Comparison with Chemical Foaming Trials

Similar to the results from the physical foaming trials, a roughly linear relation between the density and the flexural modulus and strength was observed for the chemical foaming trials. This was the case for both the materials, PPCell and PPWood, as well as for the different methods—core-back foaming with the film gate plate tool ("CB_film") or with the central gate plate tool ("CB_cent") and short-shot foaming with the film gate tool ("SSh_film"). The flexural properties of the chemically foamed samples at equal density were clearly superior to those of the physically foamed samples ("CB_phys", cf. Figure 8 for PPCell). A very similar observation was made for the Charpy notched impact strength (cf. Figure 9 for PPCell), although here the differences between the results from the physical and chemical foaming appeared slightly less prominently. The respective results for the PPWood material are shown in the Appendix A (Figures A1 and A2).
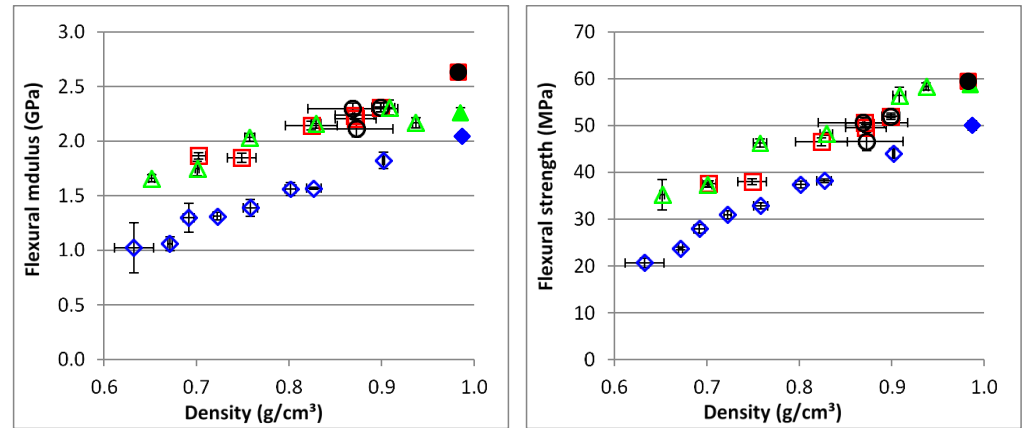
Figure 8. Flexural modulus (**left**) and strength (**right**) of PPCell, foamed with different methods. Legend: Core-back physical (N06_T60)—◇; CB_film—□; CB_cent—△; SSh_film—○. Solid symbols represent compact samples, open symbols represent foamed samples. Error bars show 95% confidence interval. If not visible, error bars lie within the size of the used symbol for the respective sample.
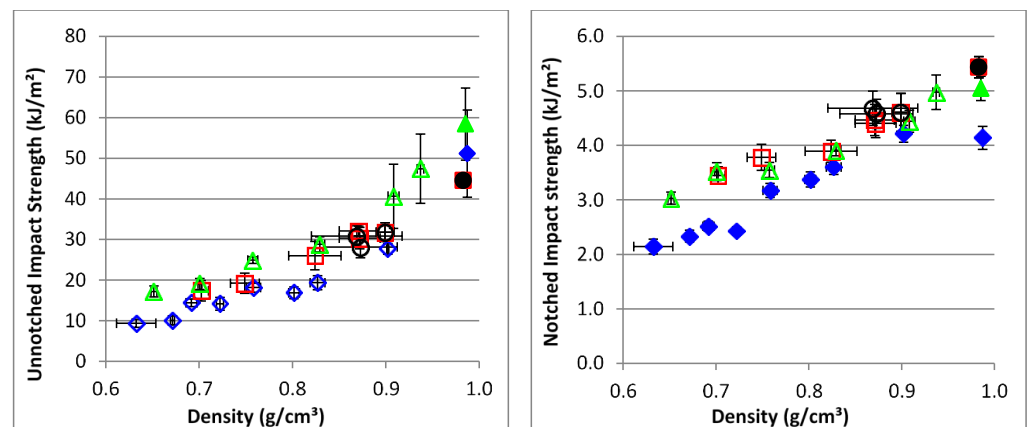
Figure 9. Charpy unnotched (**left**) and notched impact strength (**right**) of PPCell, foamed with different methods. Legend: Core-back physical (N06_T60)—◇; CB_film—□; CB_cent—△; SSh_film—○. Solid symbols represent compact samples, open symbols represent foamed samples. Error bars show 95% confidence interval. If not visible, error bars lie within the size of the used symbol for the respective sample.

Besides the different foaming techniques, one should bear in mind the different injection moulding machines that were used for the physical and chemical foaming trials, respectively, and also the use of a hot-runner system (physical trials) vs. a cold-runner system (chemical trials). In any case, the fact that all the results from the chemical trials fell approximately onto the same line shows that the plate geometry—film gate or central gate—did not appear to be a major factor in the majority of cases. The large scattering of the unnotched impact strength of the "CB_cent" samples, which occurred only in this particular series and only at low foaming degrees and in the compact sample, again indicated a non-uniform fibre orientation, as was discussed for the compact PPCell sample in the physical foaming trials (see chapter Tensile and Flexural Properties).

The flexural and impact properties of the samples prepared by short-shot foaming were comparable to those prepared by core-back foaming. However, for the short-shot samples, an interpretation of the relation between the density and the mechanical properties is less reliable because of a notable density gradient in the flow direction, which resulted in significant scattering of the data.

3.2. Optical Microscopy

In order to relate the mechanical properties to the foam structure, optical microscopic images of the cross-sections of the foamed plates were taken. The foam structures of the samples from the physical (series N06_T60) and chemical (series CB_film) foaming trials at selected mould opening gaps are shown in Figure 10 (PPWood) and Figure 11 (PPCell).
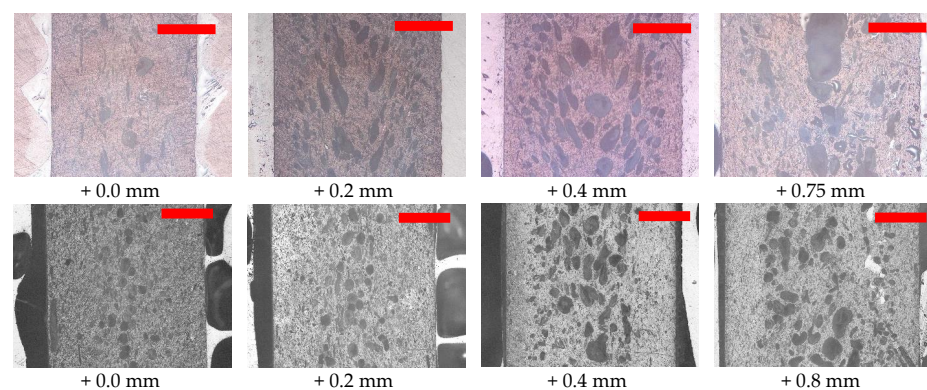
Figure 10. Foam structure of physically ((**top row**); N06_T60) and chemically ((**bottom row**); CB_film) foamed specimens of PPWood at different mould opening gaps. Dark spots in the samples represent pores, i.e., voids. Bright spots represent pores filled with resin from the sample preparation. The red bars represent 1 mm.
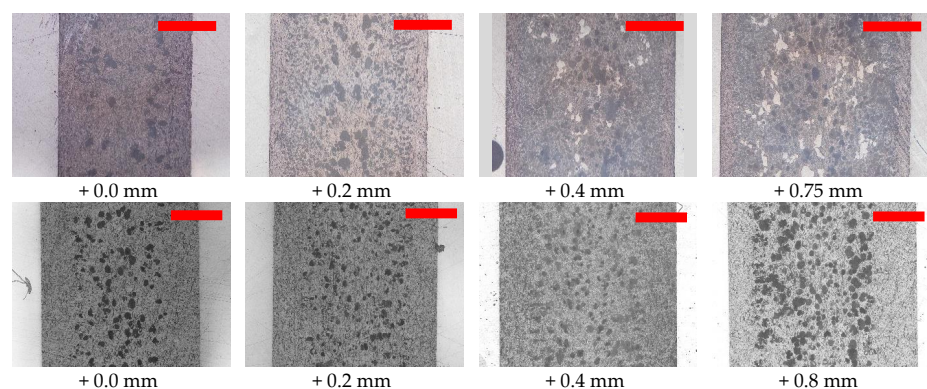
Figure 11. Foam structure of physically ((**top row**); N06_T60) and chemically ((**bottom row**); CB_film) foamed specimens of PPCell at different mould opening gaps. Dark spots in the samples represent pores, i.e., voids. Bright spots represent pores filled with resin from the sample preparation. The red bars represent 1 mm.

While there were clear differences in the foam structure not only between the two materials but also between the chemically and physically foamed samples, the evolution of the foam structure with increasing plate thickness was quite similar in all cases. Without mould opening, the foam structure seemed to consist mainly of a relatively small number of large pores. With increasing the mould opening gap, a layered structure developed where a core layer of large pores was surrounded on both sides by an intermediate layer containing a large number of small pores and a compact outer layer. With increasing the mould opening gap, the pore size increased as well, until, in the case of PPWood, even large voids of several hundred microns were formed.

A comparison of the two materials showed that the foam structure of PPCell was, in general, much finer, i.e., containing more and smaller foam cells, than that of PPWood. Since the particle size of the cellulose fibres was much smaller than that of the wood fibres, and since both compounds contained the same weight percentage of fibres, the number of filler particles per unit volume was much higher for PPCell than for PPWood. This corresponded to a larger number of nucleating sites for pore formation, which led to the observed difference in the foam structure between the two compounds. It has been reported in the literature that a smaller particle size leads to the formation of smaller foam cells [32], which supports these observations.

For both materials, the foam structure of the chemically foamed samples was finer and more homogeneous than that of the physically foamed samples. It is plausible that the chemical foaming agent, which by itself can provide nucleating sites for pore formation [19], contributed to this effect. In addition, the thickness of the compact outer layer was visibly larger for the chemically foamed samples (approx. 400–800 µm) than for the physically foamed samples (approx. 200–350 µm). Both observations were in accordance with the superior mechanical properties of the chemically foamed samples that were discussed above.

4. Conclusions

It was demonstrated that the core-back method allowed for the precise control of the part thickness in both the physical and chemical foam injection moulding trials. The roughly reciprocal correlation between the density and the part thickness and the roughly linear correlation between the tensile or flexural properties and the density showed that a constant and reproducible foaming process was achieved in all core-back trials. The simpler short-shot method led to comparable mechanical properties in relation to the density, but the results were less reproducible, which was most likely due to an inhomogeneous density distribution along the flow path.

While physical foaming appeared to be slightly more effective regarding the achievable density reduction (up to a 37% reduction), the physically foamed parts had worse mechanical properties at equal density than their chemically foamed counterparts. This could be related to the foam structure and the thicker compact outer layer that was formed in the chemically foamed samples.

The overall mechanical properties of the cellulose-reinforced compound, PPCell, were clearly superior to the wood-reinforced compound, PPWood, particularly in terms of the impact performance, which could be related to the larger aspect ratio of the cellulose fibres and also to the more homogeneous foam structure. The collected mechanical property profiles over a wide density range can serve as a basis for further optimisation trials. These are needed in order to find optimised trade-off between weight reduction and mechanical performance and thus fully exploit the weight-saving potential of foam-injection-moulded NFC composites.

Author Contributions: Conceptualisation, all authors; methodology, M.M. and C.P.; investigation, M.M. and C.P.; resources, all authors.; data curation, M.M.; writing—original draft preparation, M.M.; writing—review and editing, all authors; visualization, M.M.; supervision, C.P., T.L. and C.U.; project administration, C.P., T.L. and C.U. All authors have read and agreed to the published version of the manuscript.

Data Availability Statement: The data presented in this study are available on request from the corresponding author.

Conflicts of Interest: The authors declare no conflict of interest. The funders had no role in the design of the study; in the collection, analyses, or interpretation of data; in the writing of the manuscript; or in the decision to publish the results.

Appendix A
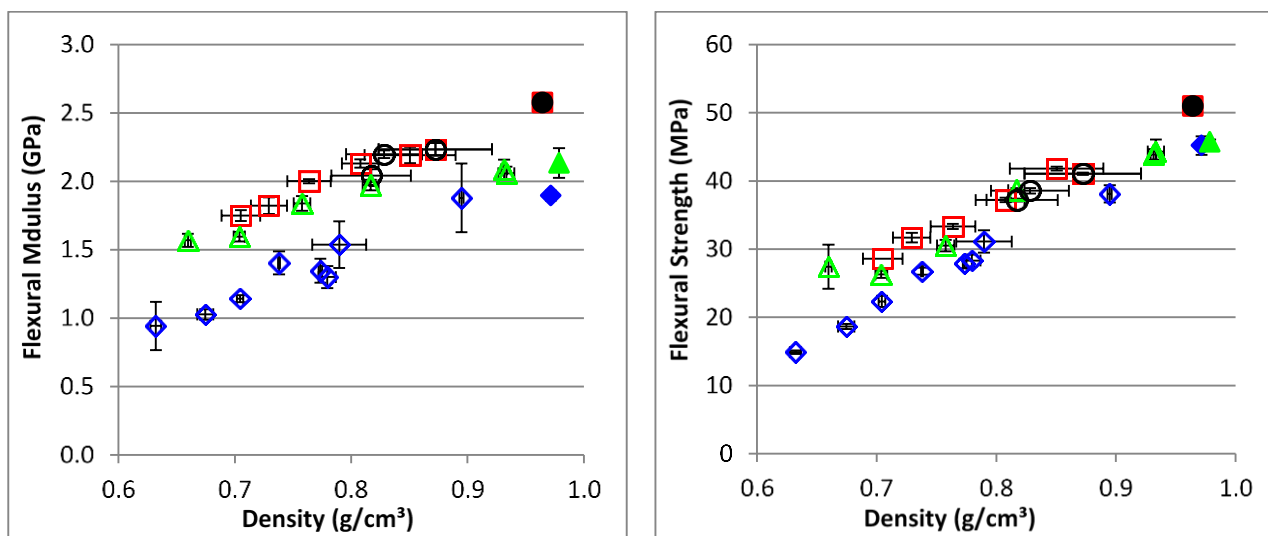
Figure A1. Flexural modulus (**left**) and strength (**right**) of PPWood, foamed with different methods. Legend: Core-back physical (N06_T60)—◇; CB_film—▢; CB_cent—△; SSh_film—〇. Solid symbols represent compact samples, open symbols represent foamed samples.
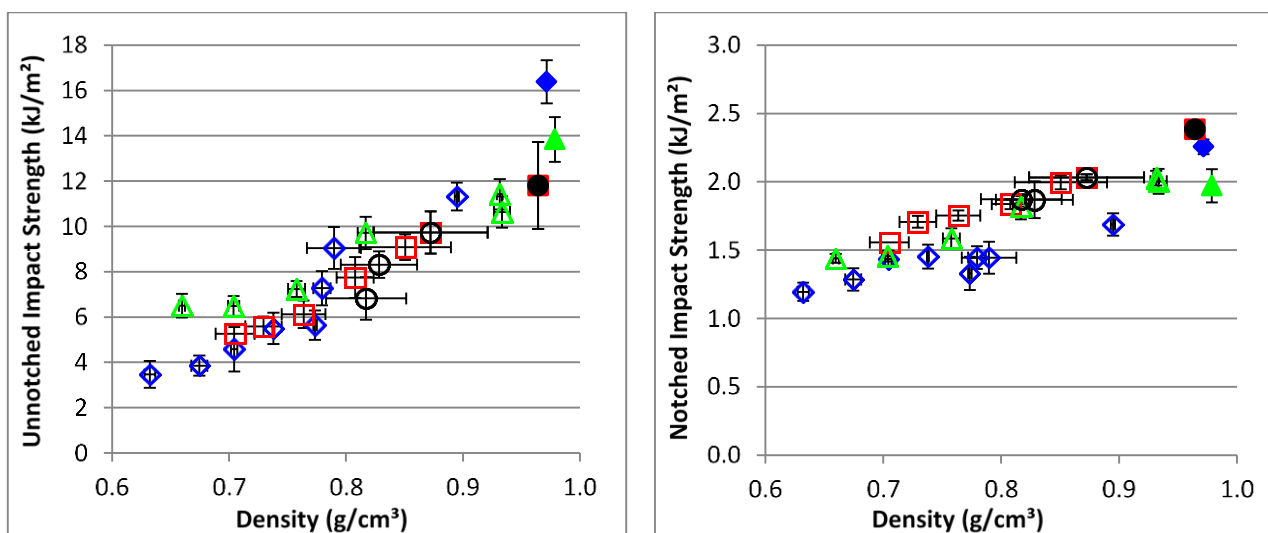
Figure A2. Charpy unnotched (**left**) and notched impact strength (**right**) of PPWood, foamed with different methods. Legend: Core-back physical (N06_T60)—◇; CB_film—▢; CB_cent—△; SSh_film—〇. Solid symbols represent compact samples, open symbols represent foamed samples.

References

1. Dufresne, A. Cellulose-Based Composites and Nanocomposites. In *Handbook of Biopolymers and Biodegradable Plastics*; Ebnesajjad, S., Ed.; William Andrew Publishing: Norwich, NY, USA, 2013; pp. 153–169. ISBN 9781455728343. [CrossRef]
2. Sobczak, L.; Lang, R.W.; Haider, A. Polypropylene Composites with Natural Fibers and Wood—General Mechanical Property Profiles. *Compos. Sci. Technol.* **2012**, *72*, 550–557. [CrossRef]
3. Civancik-Uslu, D.; Ferrer, L.; Puig, R.; Fullana-i-Palmer, P. Are functional fillers improving environmental behavior of plastics? A review on LCA studies. *Sci. Total Environ.* **2018**, *626*, 927–940. [CrossRef] [PubMed]
4. Hesser, F. Environmental advantage by choice: Ex-ante LCA for a new Kraft pulp fibre reinforced polypropylene composite in comparison to reference materials. *Compos. Part B Eng.* **2015**, *79*, 197–203. [CrossRef]
5. Badji, C.; Beigbeder, J.; Garay, H.; Bergeret, A.; Bénézet, J.-C.; Desauziers, V. Under glass weathering of hemp fibers reinforced polypropylene biocomposites: Impact of Volatile Organic Compounds emissions on indoor air quality. *Polym. Degrad. Stab.* **2018**, *149*, 85–95. [CrossRef]
6. Mihalic, M.; Sobczak, L.; Pretschuh, C.; Unterweger, C. Increasing the Impact Toughness of Cellulose Fiber Reinforced Polypropylene Composites—Influence of Different Impact Modifiers and Production Scales. *J. Compos. Sci.* **2019**, *3*, 82. [CrossRef]
7. Wang, L.; Ando, M.; Kubota, M.; Ishihara, S.; Hikima, Y.; Ohshima, M.; Sekiguchi, T.; Sato, A.; Yano, H. Effects of hydrophobic-modified cellulose nanofibers (CNFs) on cell morphology and mechanical properties of high void fraction polypropylene nanocomposite foams. *Compos. Part A Appl. Sci. Manuf.* **2017**, *98*, 166–173. [CrossRef]
8. Ding, W.; Jahani, D.; Chang, E.; Alemdar, A.; Park, C.B.; Sain, M. Development of PLA/cellulosic fiber composite foams using injection molding: Crystallization and foaming behaviors. Compos. *Compos. Part A Appl. Sci. Manuf.* **2016**, *83*, 130–139. [CrossRef]
9. Zhan, J.; Li, J.; Wang, G.; Guan, Y.; Zhao, G.; Lin, J.; Naceur, H.; Coutellier, D. Review on the performances, foaming and injection molding simulation of natural fiber composites. *Polym. Compos.* **2021**, *42*, 1305–1324. [CrossRef]
10. Ding, Y.; Hassan, M.H.; Bakker, O.; Hinduja, S.; Bártolo, P. A Review on Microcellular Injection Moulding. *Materials* **2021**, *14*, 4209. [CrossRef]
11. Lee, Y.H.; Kuboki, T.; Park, C.B.; Sain, M. The Effects of Nanoclay on the Extrusion Foaming of Wood Fiber/Polyethylene Nanocomposites. *Polym. Eng. Sci.* **2011**, *51*, 1014–1022. [CrossRef]
12. Gong, S.; Yuan, M.; Chandra, A.; Kharbas, H.; Osorio, A.; Turng, L.S. Microcellular injection molding. *Int. Polym. Proc.* **2005**, *20*, 202–214. [CrossRef]
13. Altstädt, V.; Mantey, A. *Thermoplast-Schaumspritzgießen*, 1st ed.; Carl Hanser Verlag GmbH & Co. KG: Munich, Germany, 2010. ISBN 9783446412514.
14. Lee, J.; Turng, L.S.; Dougherty, E.; Gorton, P. Novel foam injection molding technology using carbon dioxide-laden pellets. *Polym. Eng. Sci.* **2011**, *51*, 2295–2303. [CrossRef]
15. Kharbas, H.A.; McNulty, J.D.; Ellingham, T.; Thompson, C.; Manitiu, M.; Scholz, G.; Turng, L.-S. Comparative study of chemical and physical foaming methods for injection-molded thermoplastic polyurethane. *J. Cell. Plast.* **2016**, *53*, 373–388. [CrossRef]
16. Štěpek, J.; Daoust, H. Chemical and physical blowing agents. In *Additives for Plastics*; Springer: New York, NY, USA, 1983; Volume 5, pp. 112–123.
17. Kutz, M. *Applied Plastics Engineering Handbook: Processing and Materials*; Elsevier Science: Amsterdam, The Netherlands, 2011; pp. 1–574.
18. Michaeli, W.; Florez, L.; Obeloer, D.; Brinkmann, M. Analysis of the impact properties of structural foams. *J. Cell. Plast.* **2009**, *45*, 321–351. [CrossRef]
19. Ruiz, J.A.R.; Vincent, M.; Agassant, J.-F.; Sadik, T.; Pillon, C.; Carrot, C. Polymer foaming with chemical blowing agents: Experiment and modeling. *Polym. Eng. Sci.* **2015**, *55*, 2018–2029. [CrossRef]
20. Trexel, Inc. Chemical vs. Physical Foaming. Available online: https://trexel.com/chemical-vs-physical-foaming/ (accessed on 14 November 2022).
21. Standau, T.; Zhao, C.; Castellón, S.M.; Bonten, C.; Altstädt, V. Chemical Modification and Foam Processing of Polylactide (PLA). *Polymers* **2019**, *11*, 306. [CrossRef]
22. Shaayegan, V.; Wang, C.; Costa, F.; Han, S.; Park, C.B. Effect of the melt compressibility and the pressure drop rate on the cell-nucleation behavior in foam injection molding with mold opening. *Eur. Polym. J.* **2017**, *92*, 314–325. [CrossRef]
23. Ishikawa, T.; Ohshima, M. Visual observation and numerical studies of polymer foaming behavior of polypropylene/carbon dioxide system in a core-back injection molding process. *Polym. Eng. Sci.* **2011**, *51*, 1617–1625. [CrossRef]
24. Starlinger, A. *Development of Efficient Finite Shell Elements for the Analysis of Sandwich Structures under Large Deformations and Global As Well As Local Instabilities*; VDI Verlag: Duesseldorf, Germany, 1991. ISBN 318149318X.
25. Chong, T.-H.; Ha, Y.-W.; Jeong, D.-J. Effect of Dissolved Gas on the Viscosity of HIPS in the Manufacture of Microcellular Plastics. *Polym. Eng. Sci.* **2003**, *43*, 1337–1344. [CrossRef]
26. Mallick, P.K. Thermoplastics and thermoplastic-matrix composites for lightweight automotive structures. In *Materials, Design and Manufacturing for Lightweight Vehicles*; Mallick, P.K., Ed.; Woodhead Publishing: Sawston, UK, 2010; pp. 174–207.
27. Volpe, V.; De Filitto, M.; Klofacova, V.; De Santis, F.; Pantani, R. Effect of mold opening on the properties of PLA samples obtained by foam injection molding. *Polym. Eng. Sci.* **2018**, *58*, 475–484. [CrossRef]
28. Guanghong, H.; Yue, W. Microcellular Foam Injection Molding Process. In *Some Critical Issues for Injection Molding*; Wang, J., Ed.; Intech: London, UK, 2012; pp. 175–202. ISBN 9789537619992.

29. Unterweger, C.; Ranzinger, M.; Duchoslav, J.; Piana, F.; Pasti, I.; Zeppetzauer, F.; Breitenbach, S.; Stifter, D.; Fürst, C. Electrically conductive bio-composites based on poly(3-hydroxybutyrate-co-3-hydroxyvalerate) and wood-derived carbon fillers. *J. Compos. Sci.* **2022**, *6*, 228. [CrossRef]

30. Beaugrand, J.; Berzin, F. Lignocellulosic Fiber Reinforced Composites: Influence on Compounding Conditions of Defibrization and Mechanical Properties. *J. Appl. Polym. Sci.* **2013**, *128*, 1227–1238. [CrossRef]

31. Shaayegan, V. Investigation of Cell Nucleation and Growth in Foam Injection Molding through Visualization. PhD Thesis, University of Toronto, Toronto, ON, Canada, 2016.

32. Hwang, S.-S.; Hsu, P.P. Effects of silica particle size on the structure and properties of polypropylene/silica composites foams. *J. Ind. Eng. Chem.* **2013**, *19*, 1377–1383. [CrossRef]